

Chapter 7

Seismic-Monitoring Changes and the Remote Deployment of Seismic Stations (Seismic Spider) at Mount St. Helens, 2004–2005

By Patrick J. McChesney¹, Marvin R. Couchman², Seth C. Moran², Andrew B. Lockhart², Kelly J. Swinford², and Richard G. LaHusen²

Abstract

The instruments in place at the start of volcanic unrest at Mount St. Helens in 2004 were inadequate to record the large earthquakes and monitor the explosions that occurred as the eruption developed. To remedy this, new instruments were deployed and the short-period seismic network was modified. A new method of establishing near-field seismic monitoring was developed, using remote deployment by helicopter. The remotely deployed seismic sensor was a piezoelectric accelerometer mounted on a surface-coupled platform. Remote deployment enabled placement of stations within 250 m of the active vent.

Introduction

The earthquake swarm that signaled the start of the eruption at Mount St. Helens on September 23, 2004 (Scott and others, this volume, chap. 1), was recorded by a dense network of short-period stations operated jointly by the Pacific Northwest Seismic Network (PNSN), based at the University of Washington, and the U.S. Geological Survey (USGS) Cascades Volcano Observatory (CVO). The network consisted of 13 stations within 20 km of the volcano; 6 of these were within 5 km (fig. 1). Many stations had been in place since the early 1980s. Although the established monitoring was sufficient to detect the onset of the unrest, it proved inadequate to record and monitor the intense seismicity of the developing 2004–2005 eruption.

This paper recounts the changes made to the Mount St. Helens seismic network during the first year of the eruption. These include changes to the existing short-period network, the first installations of telemetered broadband seismometers, the addition of infrasonic microphones, and the remote deployment of piezoelectric accelerometers. The method of remote deployment is new—it relies on an innovative instrument package, called a “spider,” that was developed during the first month of the eruption (LaHusen and others, this volume, chap. 16). The package enabled us to safely deploy fully functional seismic stations, by helicopter, to sites within a few hundred meters of the active vent without setting a foot on the crater floor (fig. 2). Seismic spider development occurred during the response to volcanic unrest, and the following chronological sections complement the technical discussion by showing how the seismic spiders were used and how our field experiences drove the design process. Because the seismic spider uses both an uncommon sensor and unconventional deployment, we describe it at length in a subsequent section, “Technical Description of the Seismic Spiders.”

Deployment Chronology

The deployment chronology is divided into two sections. During the initial response we modified the existing short-period network and made new installations using traditional methods. Later, our focus was seismic spider deployment. To provide an overview, a summary of changes to the seismic monitoring system through 2005 is given in table 1. The instrument parameters for the spider deployments are described in a later section. The infrasonic microphones are described elsewhere (Moran and others, this volume, chap. 6).

¹ Pacific Northwest Seismic Network, Department of Earth and Space Sciences, University of Washington, Box 351310, Seattle, WA 98195

² U.S. Geological Survey, 1300 SE Cardinal Court, Vancouver, WA 98683

Initial Response to Seismic Unrest

Because Mount St. Helens was regarded as adequately monitored (Moran, 2004; Ewert and others, 2005), there was little urgency to install new instruments during the first several days of the seismic swarm that began on September 23, 2004. However, after seismicity intensified on September 26, the existing network proved inadequate in four ways (Moran and others, this volume, chap. 2): (1) The short-period network lacked dynamic range and repeatedly clipped on larger events. (2) There were no three-component instruments. (3) The network lacked the ability to record low-frequency signals. (4) There were no infrasonic sensors to record explosive activity. Consequently,

CVO and the PNSN began mobilizing to put new stations in the field. Our priorities were the installation of broadband three-component seismometers and deployment of infrasonic microphones to complement the dense short-period network.

At the same time, other cooperating groups were mobilizing to deploy broadband and strong-motion sensors with onsite recording around the volcano (Horton and others, this volume, chap. 5). However, to overcome the limited dynamic range and frequency response of the short-period network, we felt it essential to have real-time data from several broadband stations transmitted to CVO and PNSN. Because of the added complication of providing telemetry, it took several days to organize the deployment.

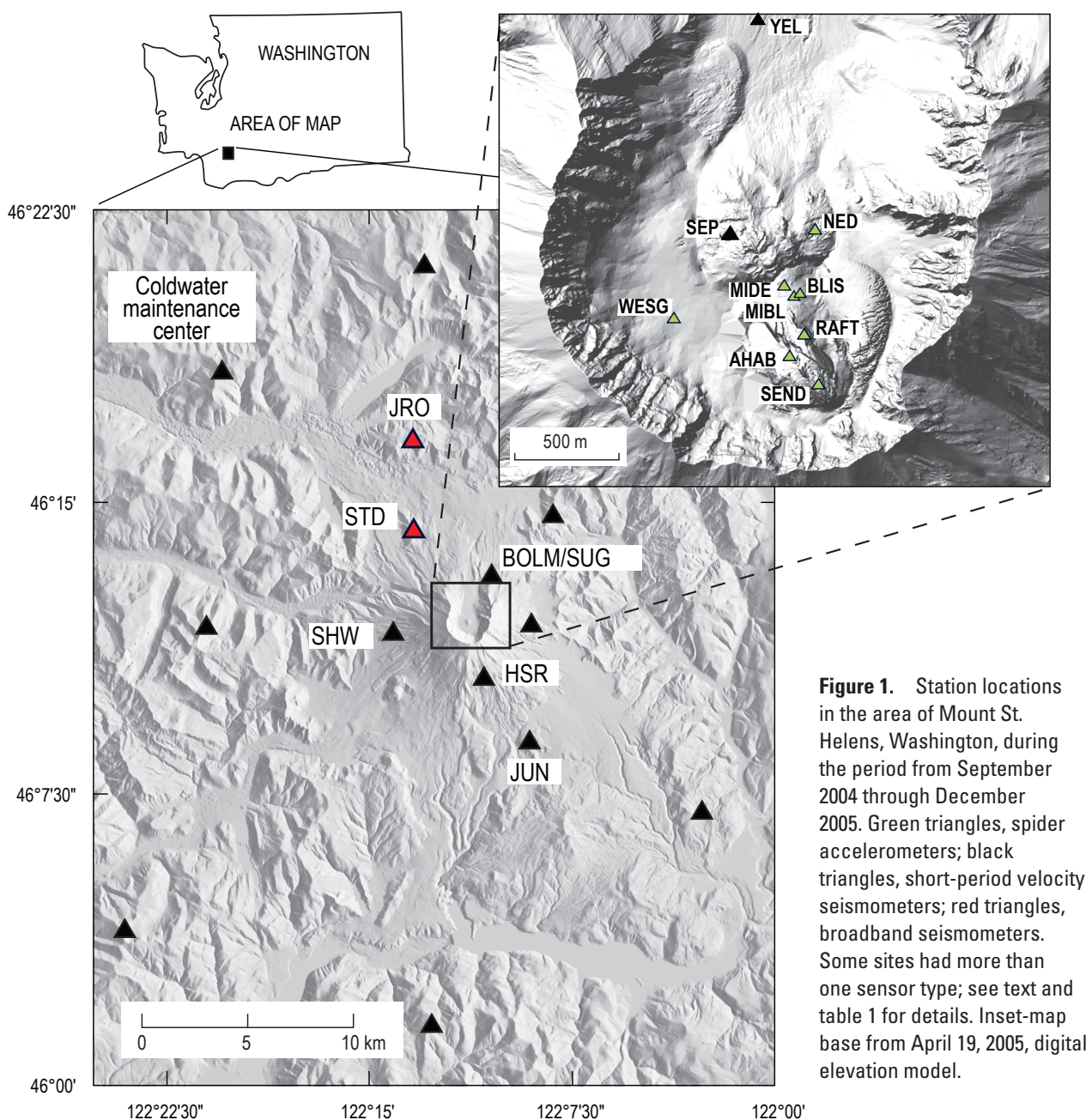


Figure 1. Station locations in the area of Mount St. Helens, Washington, during the period from September 2004 through December 2005. Green triangles, spider accelerometers; black triangles, short-period velocity seismometers; red triangles, broadband seismometers. Some sites had more than one sensor type; see text and table 1 for details. Inset-map base from April 19, 2005, digital elevation model.

On October 1, 2004, we made our first attempt to install a broadband seismometer and an infrasonic microphone at Studebaker Ridge, the site of an existing short-period station (STD; fig. 1). Work at the site, about 5 km from the vent, stopped when the first explosion of the eruption (at 1202 PDT) triggered a mandatory evacuation. As an alternative, we installed a broadband seismometer at the Johnston Ridge Observatory (JRO; fig. 1), 9 km north-northwest of the crater. Later, a broadband seismometer was successfully installed at Studebaker Ridge on October 5. Both seismometers were Guralp CMG-6TDs. These three-component instruments have a response of 30 s and were configured to measure each channel at 50 samples per second. Telemetry was not yet complete, so data were recorded initially in each instrument's 2-GB flash memory and collected later with a portable hard drive.

The interrupted installation of an infrasonic microphone at Studebaker Ridge (STDM) was completed on October 2, 2004, and another microphone (BOLM) was deployed at Sugar Bowl (fig. 1) on October 3 (Moran and others, this volume, chap. 6). The short-period seismic network was modified to provide telemetry for the microphone signals. Other changes to short-period stations were necessary in the first weeks of the eruption because signals were clipped for many earthquakes. To improve the dynamic range, a low-gain channel was added at several stations. Stations SHW and HSR were converted to dual gain on October 4 and JUN on October 7 (fig. 1). The sensitivity on the high-gain channel from HSR

was also reduced, because signals from even relatively small earthquakes were severely clipped.

Ideally the broadband instruments and microphones would have been located closer to the vent. Experience elsewhere has shown that very long period (VLP) earthquakes are best recorded on broadband instruments located within 4 km of the source region (B.A. Chouet, oral commun., 2004). By October 1, however, conditions inside the crater and on the crater rim were considered too dangerous for extended field work, so the instruments were installed more than 4 km from the source region. We will never know if VLP events occurred during the first several months of the eruption, a shortcoming that shows the importance of having at least one broadband instrument installed within 1–3 km of a potentially active vent before the beginning of unrest. None of the three explosions that occurred in the days after the October 1 event created an obvious signal on the microphones placed outside the crater (Moran and others, this volume, chap 6).

On October 20, an Earthworm data-processing node was established at the Gifford Pinchot National Forest's Coldwater Ridge maintenance facility, ~13 km northwest of the crater (fig. 1). This achievement marked a turning point in our response to the eruption by allowing Coldwater to function as a radio-telemetry terminus near the volcano. Links for the data from JRO and STD broadband seismometers were made to Coldwater with Freewave spread-spectrum digital radios (2.4 GHz). The presence of an Earthworm digitizer vastly expanded our analog channel capacity and allowed further seismic deployments to occur without long and difficult radio paths to CVO. Internet connectivity at Coldwater was through VSAT (very small aperture terminal) linked to a commercial communications network by microwave radio and satellite.

The explosion on October 1, 2004, destroyed the short-period seismic station at September lobe on the 1980–86 lava dome (SEP; fig. 1). Positioned ~500 m from the vent, SEP was the closest station to the earthquake sources. Losing this station greatly hampered earthquake location quality (Moran and others, this volume, chap. 2). The only remaining station within 3 km of the vent was the short-period station YEL (fig. 1) on the crater floor. However, the signal from YEL was clipped on many events until the gain was reduced by 12 dB during a quick visit on October 21.

Chronology of Seismic Spider Deployment

The need to reestablish near-field seismometers in the still-hazardous working conditions in the crater turned our attention to the development of a seismic station that could be deployed remotely. Available to us was the spider instrument package, originally developed for GPS deformation instruments and telemetry (LaHusen and others, this volume, chap. 16). We adapted this platform to carry an accelerometer (described in the next section) and an infrasonic microphone. The first seismic spider (BLIS, fig. 1) was deployed on October 12, 2004, at a location ~250 m east of the vent. The spider was



Figure 2. Overhead view of seismic spider deployed at station RAFT. Sensor platform (Marv lander) is at upper left. Instrument box on spider is 70 cm long. USGS photo by S.C. Moran, June 20, 2006.

Table 1. Summary of changes to preeruption seismic network at Mount St. Helens, Washington, through 2005, including infrasonic microphones.

Station	Date	Change
SEP	10/1/04	Destroyed by explosion (L4-C seismometer)
JRO	10/1/04	Guralp CMG-6TD broadband installed
STDM	10/2/04	Nine-element infrasonic microphone installed
BOLM	10/3/04	Eighteen-element infrasonic microphone installed
SHW	10/4/04	Low gain added. High gain = 60 dB, low gain = 36.5 dB (L4-C seis.)
HSR	10/4/04	Dual gain. High gain = 28 dB, low gain = -1.32 dB (S-13 seis.)
STD	10/5/04	Guralp CMG-6TD broadband installed
JUN	10/7/04	Low gain added. High gain = 60 dB, Low gain = 36.5 dB (L4-C seis.)
STDM	10/12/04	Disconnected microphone telemetry for use at station BLIS
BLIS	10/12/04	Spider with accelerometer and 18-element infrasonic microphone
YEL	10/21/04	Gain reduced by 12 dB to 54 dB (L4-C seismometer)
SEP	11/4/04	Installed L22-3D and a pair of 18-element infrasonic microphones
NED	11/20/04	Spider with accelerometer
NED	12/20/04	Spider with accelerometer on separate platform (first Marv lander)
AHAB	2/8/05	Temporary spider deployment, accelerometer, and GPS
MIDE	2/16/05	Spider with accelerometer
SEP	3/8/05	Destroyed by explosion
NED	3/8/05	Destroyed by explosion
MIDE	3/8/05	Destroyed by explosion
SUG	3/9/05	L4-C seismometer at 42 dB added to station BOLM
SEP	3/14/05	Spider with accelerometer and two 18-element infrasonic microphones
YEL	3/15/05	Gain reduced by 6 dB to 48 dB
NED	4/6/05	Reinstalled spider with accelerometer
MIDE	4/6/05	Reinstalled spider with accelerometer, reinstalled again 04/14/05
SEND	6/30/05	Spider with accelerometer
WESG	7/12/05	Temporary spider deployment, accelerometer; removed 09/14/05
MIDE	7/19/05	Destroyed by rockfall
RAFT	7/28/05	Spider with accelerometer
MIBL	11/17/05	Spider with accelerometer

remarkably successful, despite noise spikes in the seismic signal caused by radio transmissions from the co-housed GPS system. These noise spikes were eliminated by remotely turning off the GPS instrument, which had been damaged during deployment.

Volcanic and seismic activity declined substantially after October 5, 2004 (Moran and others, this volume, chap. 2). After several weeks of reduced activity, we decided it was safe to work at SEP for a short time to replace the destroyed station with a three-component seismometer and a pair of infrasonic microphones. Usually such installations take hours, but by using the spider package we thought the visit would require less than one hour. On November 4, a spider was deployed in advance of the crew. Everything required for the station was preassembled and housed in the spider except the seismometer and microphones. It took only 45 minutes to install the Sercel L22-3D three-component seismometer and two infrasonic microphones. Even so, the helicopter was forced to depart hurriedly when an ash cloud advanced on the site, just as the crew was loading the ship to leave.

The success of the spider at BLIS led to another spider deployment at the northeast corner of the old dome (NED; fig. 1) on November 20, 2004. This site was selected because it improved the geometry of stations in the crater and included a patch of warm ground that was free of snow. Data became available on November 22, after an expansion of the analog telemetry channels at the Coldwater Earthworm node.

The first NED spider worked poorly. Unlike BLIS, the seismic signal from NED was often obscured by noise. At both stations the accelerometers were mounted in a leg of the spider platform. However, NED used a heavy radome antenna mounted on a mast, whereas BLIS had used a low-mass whip antenna. Wind or ground motion shook NED's antenna and sent vibrations through the spider to the sensor. We considered using whip antennas in the future, instead of radomes, but the heavier antenna had two advantages—increased signal strength and protection from icing. In addition, we could not be certain that the antenna was the only noise source. Consequently we decided to isolate the sensor from spider vibrations

by mounting it in a separate platform, which we dubbed the “Marv lander” (see technical description in the next section). On December 23, 2004, a new spider equipped with a Marv lander was exchanged for the old one, solving the noise problem at NED.

On February 8, 2005, the spider AHAB was deployed atop the actively moving spine 4 (fig. 1). The location on the spine was chosen because it appeared stable and its slope of $\sim 20^\circ$ was not too steep for the spider. The objective of this short-term experiment was to record spine motion using GPS and to look for a correlation between “drumbeat” seismic events (Moran and others, this volume, chap. 2) and discrete movements of the spine. The spider housed an L-1 GPS receiver with an accelerometer and electronic thermometer mounted on a Marv lander. After 8 days of successful operation, AHAB was retrieved before the spine’s process of growth and collapse could destroy it.

By the end of January 2005, following a period of intermittent operation, the BLIS spider stopped operating. We were unable to find the spider because it was buried in snow. Consequently, when AHAB was removed from spine 4, it was modified in the field to become a replacement for BLIS. The new location, MIDE, was a snowfree warm spot near the BLIS site (fig. 1). Station MIDE began operation on February 16, 2005.

A small but destructive explosion occurred on March 8, 2005 (Scott and others, this volume, chap 1; Moran and others, this volume, chap. 6). Ballistic fragments from the explosion destroyed MIDE, SEP, and NED. The MIDE equipment was never found. Scattered parts of SEP were barely visible under a blanket of ash. Although NED was recovered, little could be salvaged—even the apparently undamaged accelerometer no longer functioned. The loss of these three stations severely reduced our ability to record and locate earthquakes, and the loss of the close-in microphones at SEP eliminated our ability to detect small explosions.

The first step in restoring lost monitoring capacity was the installation of a short-period seismometer just north of the crater at SUG (fig. 1) on March 9. We chose this site because of its relative safety and the fact that the Sercel L4-C seismometer could be easily connected to the existing infrasonic microphone (BOLM) telemetry. A new seismic spider, including two 1-Hz microphones, was rapidly constructed and deployed at SEP on March 14. The crater station YEL was visited on March 15 and the gain lowered by another 6 dB because of continuing clipping problems.

The weather then took a turn for the worse, delaying replacement of spiders at MIDE and NED until April 6, 2005. The NED deployment went smoothly, but the MIDE spider toppled when released by the helicopter. We retrieved and inspected it and, finding no obvious problems, returned the spider to MIDE. However, it failed several days later and was retrieved again on April 10. Several of the power system’s primary cell casings had melted, likely a result of internal damage caused by the spider’s tumble on April 6. After replacing the cells, the spider was returned to MIDE on April 14.

With the arrival of summer, more sites were free of snow and available for seismic spider deployment. On June 30, 2005, in an effort to surround the source of the drumbeat earthquakes, a spider was placed at SEND, southeast of the former AHAB installation at the southeast end of spine 4, which by then was disintegrating (fig. 1). Another installation followed at WESG (western arm of the Crater Glacier) on July 12 (fig. 1). Unfortunately, the sensitivity of WESG was poor. We suspected bad ice-rock coupling or an electronic fault. Examination after the station was retrieved showed an intermittent problem with the accelerometer interface circuit. On July 19, MIDE was destroyed by a rock fall. On July 28, 2005, a replacement spider was deployed at RAFT, the only available patch of stable ground close to the vent (figs. 1, 2).

Finally, with the approach of winter we took several steps to improve the robustness of the crater spiders. WESG was removed on September 14, 2005, before it could be buried by snow. We also retrieved all spiders except RAFT to replace batteries and, if necessary, to add directional antennas. Subsequently, ice accumulation from an early winter storm damaged the coaxial cable for the radio transmitter at SEND. The SEND spider was retrieved and repaired on November 17. Because earthquakes had become much smaller, we relocated this spider to a new site, MIBL, closer to the vent (fig. 1). The MIBL site was warm and free of snow and near the previous MIDE and BLIS sites.

By the end of 2005, the CVO and PNSN real-time seismic network at Mount St. Helens consisted of 2 broadband seismometers, 13 conventional short-period instruments (3 with dual-gain channels), 4 seismic spiders, and 2 infrasonic microphones, all within 20 km of the volcano (table 1).

Technical Description of the Seismic Spiders

The loss of SEP during the explosion of October 1, 2004, forced us to improvise new techniques in order to restore seismic monitoring near the vent. Particularly for the first installations, we hurried to get something in the field, and each deployment was an experiment that led to changes in design. The evolving design complicates the description of the spider, because it is necessary to include the changes that were made. We trust that this section gives sufficient detail to satisfy both those who need to know the response parameters for a spider installation and those who are considering the design of remotely deployed seismic instruments.

Seismic Spider Overview

We designed the seismic spider for remote deployment close to an active volcanic vent where seismic signals were strong. Remote deployment ruled out the use of traditional seismic sensors, which require leveling by hand during instal-

lation. We knew of a sensor, used for measuring seismic activity of lava flowing through tubes in Hawai'i (R. Hoblitt, oral commun., 2004), that did not require leveling, could measure strong signals, and could survive the rigors of remote deployment. This sensor, a piezoelectric accelerometer, made the seismic spider possible.

Analog telemetry was used for a variety of reasons. Given strong signals, the contribution of some noise by the analog telemetry system did not detract much from the overall signal-to-noise ratio. The limited dynamic range of the telemetry system was overcome by using high- and low-gain channels. Analog telemetry allowed the use of lower frequency analog radios that, unlike digital spread-spectrum radios, do not require line-of-sight transmission paths and use much less power. The radios operated on the 406 to 420 MHz band, where antennas are fairly compact and their 100-mW transmissions can cover tens of kilometers. Several antennas were tried, but high-gain directional antennas were preferred because the radio path was often obstructed by ter-

rain or snow. To prevent breakage from snow and ice loading, radome-protected antennas were favored.

Power was supplied by Air-Alkaline primary cells (Celair Corp.). Nine series-connected cells provided 12.6 V at 1,200 Ah. Total current drain was 110 mA, so 450 days of continuous operation were possible, but we planned for no more than a year because of capacity loss in cold weather.

The spider instrument package, developed early in this eruption to remotely deploy GPS instruments (LaHusen and others, this volume, chap. 16), provides an instrument compartment ($\sim 70 \times 40 \times 40$ cm) optimized for helicopter transport and placement (fig. 3). We used the spider to house the power and telemetry systems and, initially, the sensor. Because of noise problems with the first two deployments, the sensor was moved to a separate platform, the Marv lander (described below).

Piezoelectric Accelerometer

Long used by industry for machine vibration measurement, piezoelectric accelerometers do not require leveling because they operate in any orientation. These devices convert dynamic forces to electrical energy through charge separation in a piezoelectric material. Acceleration (a) along the axis of the transducer acts on the seismic mass (M) to apply a force to the piezoelectric element. The force on the element produces a charge (q) such that $q = dMa$, where d is the piezoelectric constant. The stressed piezoelectric material acts as a capacitor (C), producing an open-circuit voltage (V) where $V = q/C$. Consequently the sensitivity of the accelerometer is V/g , where g is the unit of acceleration (Allocca and Stuart, 1984, p. 122).

Piezoelectric accelerometers respond to dynamic forces—to vibrations. The circuit model is a current generator in parallel with a capacitor, or its equivalent circuit, a voltage generator in series with a capacitor (Allocca and Stuart, 1984, p. 122–123). The model shows that there is an inherent low-frequency limit to a piezoelectric accelerometer. In addition, low-frequency vibrations produce weak acceleration signals, so piezoelectric accelerometers operating at low frequencies must use charge amplifiers to boost signal levels. The low-noise design of this amplifier is critical for low-frequency measurements because noise from the high input resistance of the charge amplifier increases with decreasing frequency (Schloss, 1993, p. 2). Consequently, poor signal-to-noise ratios at low frequency set the practical limit of piezoelectric response.

Sensor Parameters

We chose the Wilcoxon Model 731-207 Ultra Low Frequency Seismic Accelerometer for this application because of its relatively good low-frequency performance (see abbreviated specifications in table 2). There are other piezoelectric accelerometers with better low-frequency specifications than this model, but there is a tradeoff between increased low-



Figure 3. Seismic spider slung by helicopter from staging area on March 14, 2005, for deployment at SEP. Included are two infrasonic microphones, one suspended immediately beneath the spider and another below it on the lander sensor platform (Marv lander), last item in the string. PNSN photo by P.J. McChesney, March 14, 2005.

frequency response and increased fragility. Because the sensors are subject to significant forces during deployment, the 250 g shock limit of the Model 731-207 was attractive. All units survived our handling and the helicopter deployment. However, one unit from NED, recovered after the explosion of March 8, 2005, was irreparably damaged, probably from ballistic impact.

The peak acceleration range of this model is more than sufficient for close-in monitoring. The low-gain telemetry channel was set for a maximum measurement of 0.1 g, a limit that was never exceeded despite recording M_L 3.4 earthquakes within 250 m of the source. The high sensitivity of the device permitted conservative seismic amplifier gain settings. Two telemetry channels were used for high- and low-gain recordings of the signal, with the low-gain channel set at 2.5 V/V. The high-gain channel was initially set at 83.17 V/V but was reduced to 41.75 V/V for later deployments. In the absence of noise, these gain settings achieve 16-bit dynamic range using two analog telemetry channels digitized at 12 bits each.

Response information for individual sensors is unavailable from the manufacturer. The nominal frequency response at 0.2 Hz is a worst-case limit. The design value for the low-frequency cutoff (−3 dB) is 0.1 Hz. This high-pass response has a pole at (−0.628319, 0) and a zero at (0, 0) set by charge amplifier components. Actual response is determined by component variation, and any particular unit may have a pole frequency from 0.1 to 0.15 Hz (Ron Denton, Application Engineer, Wilcoxon Research, written commun., 2006).

We attempted continuous electronic integration of the accelerometer output to produce a velocity response. Even though integration in the field was not satisfactory, it demonstrated the noise characteristics of the sensor. The data sheet for the Model 731-207 states that spectral noise, a 1-Hz bandwidth noise-density measurement at a particular frequency (Schloss, 1998, p. 1), increases as frequency decreases. At 2 Hz the noise density is 0.28 g/Hz. However, integration provides gain relative to the acceleration response; gain increases by a factor of two each time frequency is halved. In addition, below 2 Hz, sensor noise increases as $1/f$ (Ron Denton, Application Engineer, Wilcoxon Research, written commun., 2005). The combination of decreasing signal-to-noise ratio and increasing gain causes low-frequency noise to be prominent in the integrated response. Analog filtering of the low-frequency noise interfered with the integrator phase response. On the other hand, the acceleration response of the sensor has very good noise performance. Consequently the acceleration response was telemetered because we felt that digital postprocessing could do a better job if the velocity response was desired.

Piezoelectric Accelerometer Interfacing

The charge amplifier in the accelerometer can produce high-amplitude signals (5 V) and requires a power source. The voltage-controlled oscillators (VCOs) used to telemeter seis-

Table 2. Abbreviated specifications for the Wilcoxon Model 731-207 piezoelectric accelerometer.

[Additional information online at www.wilcoxon.com.]

Accelerometer Specifications	
Sensitivity	10 V/g, $\pm 10\%$, 25°C
Acceleration Range	± 0.5 g
Frequency Response	0.2–1300 Hz, −3 dB
Resonance Frequency	2,400 Hz
Temperature Response	−18% at 0°C, +8% at 80°C
Broadband Noise	2 μ g, 2.5 Hz to 25 kHz
Input Voltage Range	18–30 VDC, in series with a 2–10 mA current source diode
Shock Limit	250 g

mic signals are usually connected to passive seismometers that produce small-amplitude signals in the millivolt range. This mismatch required an interface circuit and VCO gain adjustments. We used McVCO, a microcontroller-based mimic of an analog VCO (McChesney, 1999). The interfacing problems are similar for other VCOs, but the details are best appreciated if the McVCO documentation is at hand.

The Model 731-207 accelerometer is a two-wire device. There is a ground connection and a combined signal and power connection. Power is provided through a current-source diode in series with a DC supply of 18–30 V. The signal rides on a 10-V bias. The most straightforward way to connect the accelerometer to the VCO is to raise the impedance of one VCO input and make a single-ended connection through a coupling capacitor. The nominal 24-V power required by the accelerometer can be generated from the 12-V telemetry power system with a voltage-doubler circuit.

This approach was used for the first deployments at BLIS and NED. The coupling capacitor at the VCO input produced a high-pass pole at 0.047 Hz, well below the nominal 0.2-Hz charge amplifier pole in the accelerometer. To achieve this low frequency, tantalum electrolytic capacitors were used. However, investigation of noise problems with the first NED deployment indicated that some sudden baseline shifts were due to the capacitor. The second deployment at NED used a polypropylene capacitor and higher input resistance to produce a pole at 0.04 Hz.

The polypropylene capacitor appeared to reduce some noise problems, but the design was still bothered by the spikes that occurred when GPS and seismic instruments cohabited the same spider. This and an interest in electronic integration of the accelerometer signal provoked the development of a different interface (fig. 4). The new interface used an input buffer to raise the impedance and a differential output stage that allowed connection directly to an unmodified VCO input. Rather than use a 24-V supply, the sensor ground was operated at −12 V, putting the output offset at −2 V and eliminating the need for a coupling capacitor at the sensor output. An optional integration stage was provided.

A high-pass pole (R4, C16) is included in the interface after the buffer stage. This was initially set to 0.017 Hz, making the charge amplifier pole dominant at low frequencies and reducing interaction with the optional integrator. This was later raised to 0.17 Hz when some low-frequency noise problems were seen in the accelerometer response. It has not been possible to duplicate this noise; it may have been unique, but for the sake of uniformity the pole continues to be set at 0.17 Hz. Table 3 lists deployment interface response characteristics and gains. Poles and zeros are from circuit simulation. All responses more than ten times the 30-Hz VCO low-pass filter are ignored.

This interface has been used for all our piezoelectric accelerometer deployments starting with the deployment of AHAB on February 8, 2005, and continuing through 2005, but it could be improved. Cohabitation with GPS still produces small glitches in the seismic signal when the GPS

data transmission occurs. We expect that GPS noise could be reduced further by locating the interface on the sensor platform (fig. 3). This would change the connection in the long cable between the lander and the spider from a high impedance single-ended connection to a lower impedance differential connection. Better supply regulation might also help eliminate noise.

Gain Setting

The gain model for the dual-gain mode we used for all seismic spiders is shown in figure 5. Maximum acceleration of the Model 731-207 produces a maximum signal level of 5 V. This is greater than the input range of the McVCO, so the signal is reduced by half in all versions of the interface. The gain of two, created by the differential connection of the

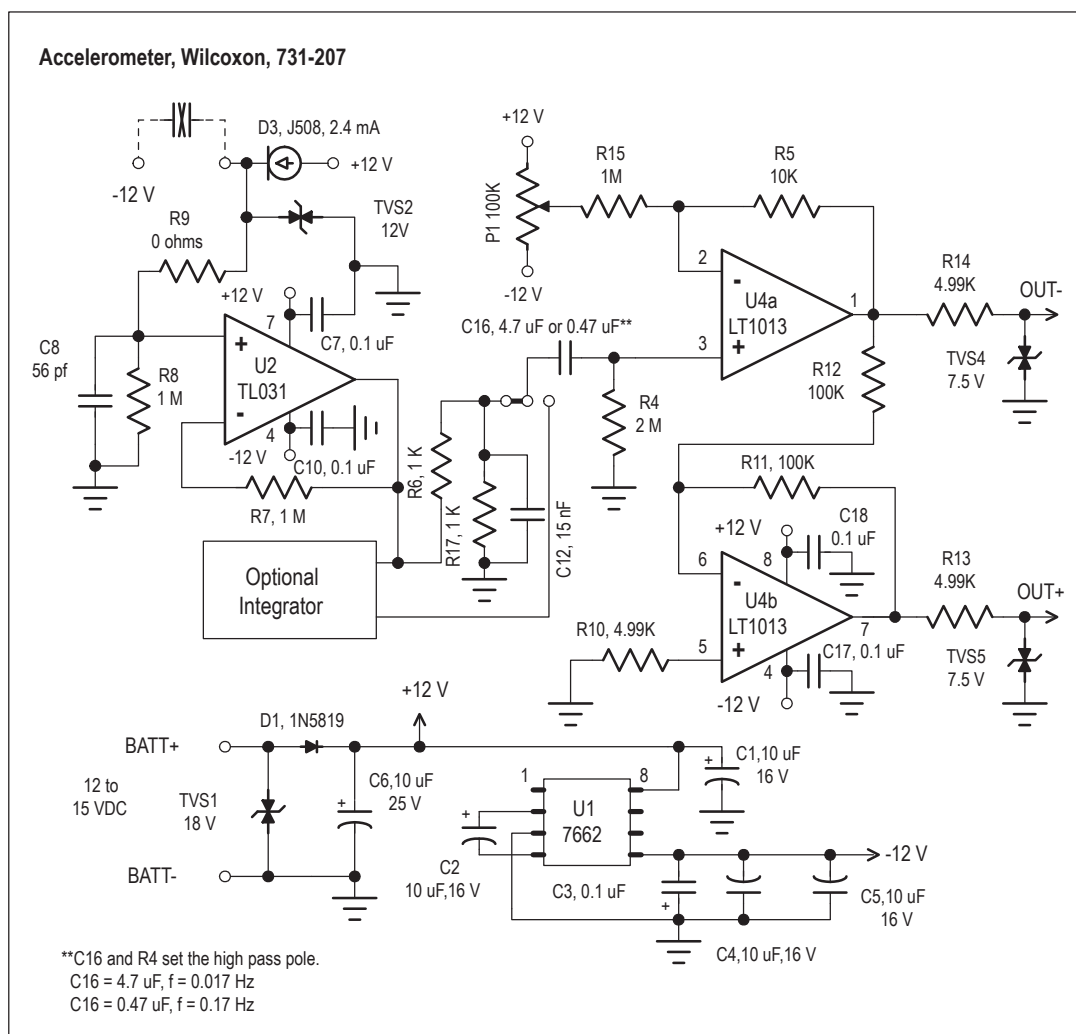


Figure 4. Piezoelectric accelerometer interface used from February 8, 2005, onward. Low-frequency response controlled by C16 and R4.

Table 3. Piezoelectric accelerometer channel gains and interface frequency responses.

[Different deployments to the same location are indicated by numerals in parentheses in station column. Last date for each station entry indicates modification or end of operation. nc, no change.]

Station	Date	High gain V/V	Low gain V/V	Interface response (poles), (zeros)
BLIS	10/12/04	83.17	2.5	(−0.294685, 0), (0, 0)
lost	01/31/05	--	--	--
NED(1)	11/20/04	83.17	2.5	(−0.294685, 0), (0, 0)
exchanged	12/20/04	--	--	--
NED(2)	12/20/04	83.17	2.5	(−0.249969, 0), (0, 0)
destroyed	03/08/05	--	--	--
AHAB	02/08/05	41.75	2.5	(−0.106357, 0), (0, 0)
removed	02/16/05	--	--	--
MIDE(1)	02/16/05	41.75	2.5	(−0.106357, 0), (0, 0)
destroyed	03/08/05	--	--	--
SEP	03/14/05	41.75	2.5	(−0.106357, 0), (0, 0)
modified	10/18/05	nc	nc	(1.06357, 0), (0, 0)
NED(3) modified	04/06/05	41.75	2.5	(−0.106357, 0), (0, 0)
	10/18/05	nc	nc	(−1.06357, 0), (0, 0)
MIDE(2)	04/06/05	41.75	2.5	(−0.106357, 0), (0, 0)
destroyed	07/19/05	--	--	--
SEND	06/30/05	41.75	2.5	(−1.06357, 0), (0, 0)
removed	11/17/05	--	--	--
WESG	07/12/05	41.75	2.5	(−1.06357, 0), (0, 0)
removed	09/14/05	--	--	--
RAFT	07/28/05	41.75	2.5	(−1.06357, 0), (0, 0)
MIBL	11/17/05	41.75	2.5	(−1.06357, 0), (0, 0)

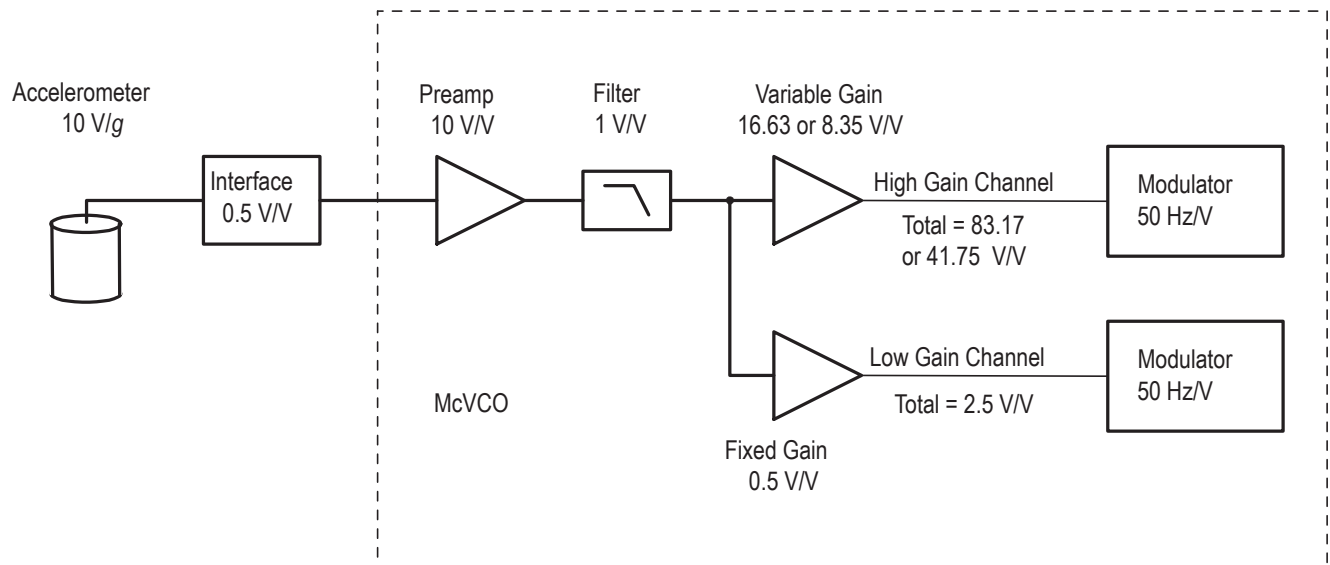


Figure 5. Dual-gain model of spider accelerometer. Additional gain and response terms result from demodulation and digitization. McVCO, microcontroller-based mimic of analog voltage-controlled oscillator.

later interfaces, is cancelled by the attenuation caused by the impedance match between interface and VCO, so the net gain of all interface stages is 0.5 V/V.

The input amplifier in the McVCO usually has a gain of 100 V/V. This was reduced to 10 V/V with jumpers on the input stage (McChesney, 1999, p. 31). After filtering (4th-order Butterworth, low-pass, 30-Hz filter) the signal splits into low- and high-gain channels. The low-gain channel is modified to have a gain of 0.5 V/V after the filter; consequently the total gain is 2.5 V/V from the interface input to the low-gain channel output. The maximum input signal swing of the channel's analog to digital converter is 2.5 V. A signal of 1 V from the sensor (0.1 g) produces a full-scale measurement on the low-gain channel.

The amplification of the high-gain channel after the filter stage depends on the gain switch setting and the microcontroller program version (McChesney, 1999, p. 15, p. 30–31). The high-gain channel after the filter stage was initially set for 16.63 V/V for a total gain of 83.17 V/V from the interface input to the high-gain channel output. As stated previously, this was reduced to 8.35 V/V for a total gain of 41.75 V/V for the deployments from AHAB onward (see table 3).

The McVCO modulator sensitivity is 50 Hz/V (McChesney, 1999, p. 30–31). The sensitivity of the discriminators used for demodulation was 0.02 V/Hz. The digitizer sensitivity was 819.2 counts/V. Where the total response to input excitation is the quotient of output counts divided by acceleration input, the scale factor for each channel voltage gain is shown in table 4.

Table 4. Scale factor for accelerometer channel gains.

Channel gain, V/V	Scale factor, counts/g
2.5	20,480
41.75	342,016
83.17	681,329

The “Marv Lander” Platform

We discovered a significant noise problem caused by spider vibrations during the first NED deployment. Later testing showed that soft tapping anywhere on the spider generated high levels of noise as long as the accelerometer was mounted on it. Our solution was to put the sensor on a separate platform, the “Marv lander,” named for its developer, Marvin Couchman.

Previous experience with seismic installations at Mount St. Helens had shown that it was not always necessary to bury a seismometer to get good coupling and good noise performance. The installation at SEP before October 2004 was such an example. At the SEP site, warm temperatures a few centimeters below ground had caused rapid failures of several Sercel L4-C seismometers before a surface installation solved the problem.

This approach was continued with the Sercel L22-3D installation at SEP on November 4, 2004. Other experiences with installations on rock, where digging was impossible, had also produced favorable results. In all these cases, isolation from surface noise was achieved by surrounding the seismometer with a rock pile, bags of sand, or concrete. We reasoned that a seismometer platform for remote deployment should provide significant mass around the sensor. Consequently the lander body is a 20-kg barbell weight (45 lb) with the piezoelectric sensor sealed with epoxy in the center hole (fig. 6).

The platform is coupled to the ground through three short legs formed by the eyebolts used to attach the rigging between it and the spider. Most of the spider sites had some ash cover, and, although we could not closely observe most of the platforms on the ground, we believe that the combination of tripod legs and weight helped root them in the ash and avoid tipping instability. The barbell weight also provided thermal mass, isolating the piezoelectric sensor from temperature changes rapid enough to produce an inband signal.

The lander rigging includes a 5-m length of 5-mm ($3/16$ in.) stainless steel cable attached to the spider's instrument box with a ring and thimble that protect the cable from wear during the helicopter flight (fig. 7). At the other end, a 10-mm ($3/8$ in.) rope harness attaches the lander to the cable. Soft rope is used to isolate the cable from the lander, eliminating cable vibrations as a source of seismic noise. Polypropylene rope was used for the first lander. When the instrument was retrieved after an explosion, one of the three leads was burned through, and hot rock was found embedded in the others. Subsequently, nylon rope was used because of its higher melting point and superior strength.

Separating the sensor from the spider body created some electrical problems. When the seismic spider is set down by the helicopter, the lander makes first contact with the ground. This can produce a strong static discharge between the lander

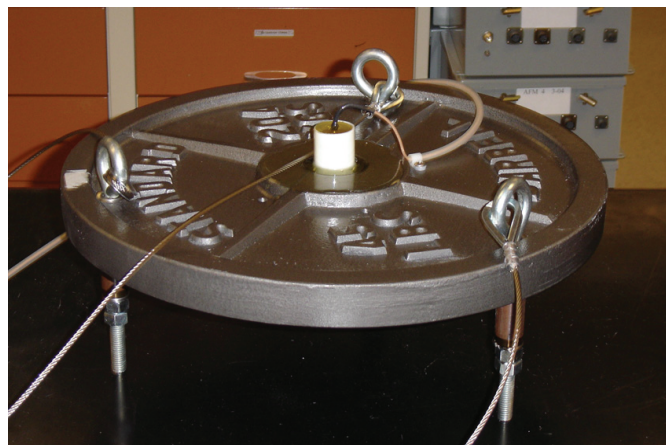


Figure 6. Marv lander under construction. Barbell weight stands on three legs formed by eyebolts that connect with rigging. Accelerometer is potted with epoxy inside the plastic pipe, which is cemented into center of the weight. USGS photo by M.R. Couchman, December 2, 2004.

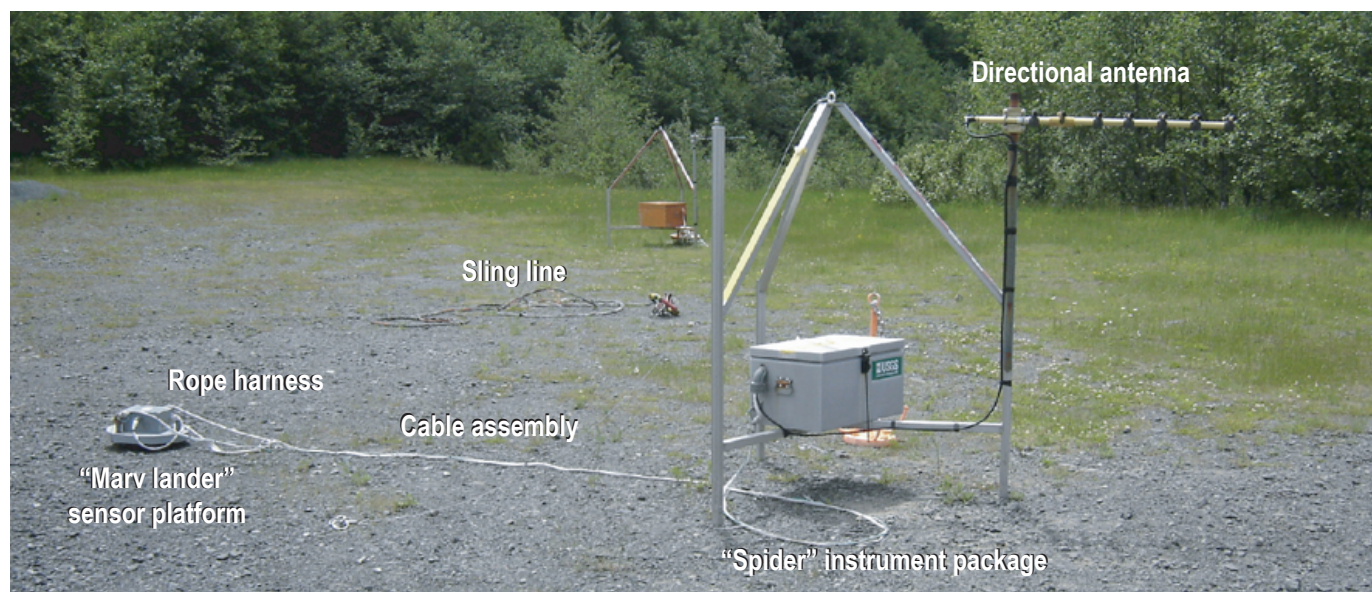


Figure 7. Seismic spider laid out at staging area. Instrument box is approximately 70x40x40 cm. USGS photo by S.C. Moran, June 20, 2006.

and the spider that can damage the sensor and electronics. To provide a low-impedance discharge path, a grounding wire connects one of the lander's legs to the spider body. Discharge through the signal-cable shield is avoided by grounding it only at the spider end, and the sensor case is isolated from the lander body by potting it with epoxy inside a short length of PVC pipe (fig. 6). The signal cable is vulnerable to thermal and mechanical damage. Consequently, the two-pair shielded cable (Belden type 8723) is enclosed in thermal sleeving. Grounding wire and sensor cable are tied to the lander rigging.

The performance of an accelerometer mounted on the lander is illustrated in figure 8. The top trace is from the piezoelectric accelerometer installation at SEP shortly before it was replaced by a three-component velocity seismometer (Sercel L22-3D) on February 24, 2006. The bottom trace is from the L22 and shows an earthquake from February 26, 2006. The two earthquakes were chosen because signals from other stations indicated that they were very similar, having approximately the same magnitude, location, and source mechanism. The accelerometer data were integrated to produce a velocity response and then filtered (2 Hz, Butterworth high-pass filter) to remove long-period noise and produce an instrument response comparable to the L22. Despite the fact that the two sensor locations differed by ~15 m, their seismic traces share many similarities, particularly at the onsets. More to the point, the comparable signal-to-noise ratios show the effectiveness of the lander coupling.

Summary

Even though Mount St. Helens was regarded as a well-monitored volcano, the September 2004 unrest exposed weaknesses in the seismic monitoring network. The explosion of October 1,

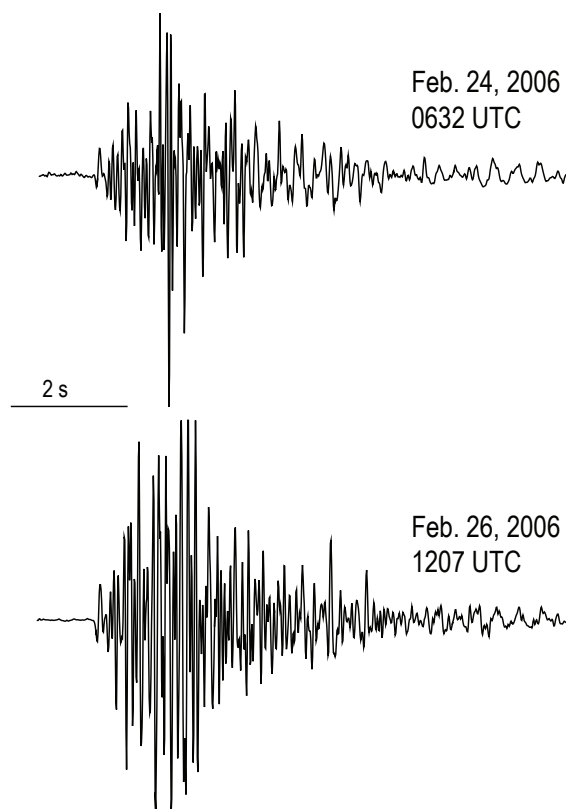


Figure 8. Comparison of numerically integrated response of piezoelectric accelerometer (top) and velocity seismometer (bottom) for similar earthquakes at station SEP. Accelerometer data were integrated to produce a velocity response and then filtered to remove long-period noise and produce an instrument response comparable to the velocity seismometer.

2004, removed our near-field monitoring capacity when station SEP was lost, reducing the quality of hypocenter determinations. One or more additional close-in stations would have increased the chance that near-field monitoring could survive a small explosion. Deployment of broadband seismometers before the start of volcanic unrest would have supplemented the short-period network by making up for its limited dynamic range and, if positioned within 4 km, could have detected any very long period events.

Once the eruption started, near-field sites quickly became too dangerous for fieldwork. However, with the seismic spider, we were able to improvise a solution that allowed us to establish close-in sites in comparative safety. The spider package not only enabled us to place a telemetered seismometer close to the vent but also to retrieve it for service or redeployment. This portability facilitated short-term studies such as AHAB on spine 4, and portability allowed us to adapt to changing field conditions during this prolonged eruption. A different choice of sensor and telemetry technology for remote deployment might have emerged from a less-hasty development process, but, given the advantage of strong signals in the near-field, both the sensor and analog telemetry were more than adequate for the task. We were particularly pleased with the performance of the Marv lander. It eliminated the spider platform noise and produced good coupling for the sensor. With the possible exception of the glacier site (WESG), there were no signal problems caused by poor sensor installation in 10 deployments.

Seismic spiders are not substitutes for well-established seismic stations because they lack the sensitivity to detect small earthquakes, unless they happen to be in the near field, or to detect the long-period earthquakes that may well mark the start of volcanic unrest. However, once unrest has begun, they can be used to supplement an existing network where additional near-field monitoring is desired. These portable, remotely deployed stations can be built in advance, allowing a very rapid response to events. The seismic spider is a new tool for monitoring erupting volcanoes, a tool that can be used in dangerous places with comparative safety.

Acknowledgments

The authors would like to thank Richard P. Hoblitt for suggesting the piezoelectric accelerometer used in the seismic spider and supplying them during the first deployments. His perceptive review of this paper greatly increased its coherence. Thomas L. Murray's review gave us a new perspective on the seismic spider design; this resulted in a more balanced paper and allowed us to avoid several shortcomings. Finally, we would like to thank Anthony Qamar for his initial calculation of the peak acceleration that a near-field sensor would measure and his many discussions of instrument response. Because of Tony, seismic spider data were "on scale" and calibrated.

References Cited

- Allocca, J.A., and Stuart, A., 1984, *Transducers—theory and applications*: Reston, Va., Reston Publishing Company Inc., 497 p.
- Ewert, J.W., Guffanti, M., and Murray, T.L., 2005, An assessment of volcanic threat and monitoring capabilities in the United States; framework for a National Volcano Early Warning System: U.S. Geological Survey Open-File Report 2005–1164, 62 p.
- Horton, S.P., Norris, R.D., and Moran, S.C., 2008, Broadband characteristics of earthquakes recorded during a dome-building eruption at Mount St. Helens, Washington, between October 2004 and May 2005, chap. 5 of Sherrod, D.R., Scott, W.E., and Stauffer, P.H., eds., *A volcano rekindled; the renewed eruption of Mount St. Helens, 2004–2006*: U.S. Geological Survey Professional Paper 1750 (this volume).
- LaHusen, R.G., Swinford, K.J., Logan, M., and Lisowski, M., 2008, Instrumentation in remote and dangerous settings; examples using data from GPS "spider" deployments during the 2004–2005 eruption of Mount St. Helens, Washington, chap. 16 of Sherrod, D.R., Scott, W.E., and Stauffer, P.H., eds., *A volcano rekindled; the renewed eruption of Mount St. Helens, 2004–2006*: U.S. Geological Survey Professional Paper 1750 (this volume).
- McChesney, P.J., 1999, McVCO handbook 1999: U.S. Geological Survey Open-File Report 99–361, 48 p. [<http://wrgis.wr.usgs.gov/open-file/of99-361/>, last accessed Dec. 26, 2006].
- Moran, S.C., 2004, Seismic monitoring at Cascade volcanic centers, 2004; status and recommendations: U.S. Geological Survey Scientific Investigations Report 2004–5211, 28 p.
- Moran, S.C., Malone, S.D., Qamar, A.I., Thelen, W.A., Wright, A.K., and Caplan-Auerbach, J., 2008a, Seismicity associated with renewed dome building at Mount St. Helens, 2004–2005, chap. 2 of Sherrod, D.R., Scott, W.E., and Stauffer, P.H., eds., *A volcano rekindled; the renewed eruption of Mount St. Helens, 2004–2006*: U.S. Geological Survey Professional Paper 1750 (this volume).
- Moran, S.C., McChesney, P.J., and Lockhart, A.B., 2008b, Seismicity and infrasound associated with explosions at Mount St. Helens, 2004–2005, chap. 6 of Sherrod, D.R., Scott, W.E., and Stauffer, P.H., eds., *A volcano rekindled; the renewed eruption of Mount St. Helens, 2004–2006*: U.S. Geological Survey Professional Paper 1750 (this volume).
- Schloss, F., 1993, Accelerometer noise: Gaithersburg, Md., Wilcoxon Research, Inc., Sound and Vibration instrumentation reference issue, March 1993, 2 p. [<http://www.wilcoxon.com/knowdesk/accelnoise.pdf>, last accessed Dec. 26, 2006].
- Schloss, F., 1998, Piezoelectric accelerometer specifications and specmanship: Gaithersburg, Md., Wilcoxon Research, Inc., Sound and Vibration, February 1998, 2 p. [http://www.wilcoxon.com/knowdesk/piezo_spec.pdf, last accessed Jan. 8, 2007].
- Scott, W.E., Sherrod, D.R., and Gardner, C.A., 2008, Overview of 2004 to 2006, and continuing, eruption of Mount St. Helens, Washington, chap. 1 of Sherrod, D.R., Scott, W.E., and Stauffer, P.H., eds., *A volcano rekindled; the renewed eruption of Mount St. Helens, 2004–2006*: U.S. Geological Survey Professional Paper 1750 (this volume).